Simultaneous Wireless Transmission Based on Visible LED of On-Off-Keying and Discrete Multitone Signal Using Sparse Compressive Sampling and Derivative-Subtractive Sampling

Yong-Yuk WON [1], Sang Min YOON [2]

[1] Dept. of Electronic Engineering, Myongji University 116 Myongji-ro, Cheoin-gu, Yongin, Gyeonggi-do, 17058, Korea
[2] College of Computer Science, Kookmin University, 77 Jeongneung-ro, Seoul, 02707, Korea

bluejerry@mju.ac.kr, smyoon@kookmin.ac.kr

Submitted July 6, 2022 / Accepted September 30, 2022 / Online first October 27, 2022

Abstract. *We propose a technique for simultaneously transmitting two signals with different waveforms, non-return-to-zero on-off keying (NRZ-OOK) signal and discrete multi-tone (DMT) signal, in an optical wireless link based on visible light emitting diode (LED). A sparse compressive sampling technique is proposed to reduce the length of the DMT signal encoded by quadrature phase shift keying (QPSK) symbols and a derivative-subtractive sampling is proposed to separate the NRZ-OOK signal and the DMT signal from the mixed signal (NRZ-OOK + DMT). It is possible to reduce the length of the DMT signal up to 38% using the sparse compressive sampling technique. A 37.6-Mb/s transmission capacity (NRZ-OOK: 10 Mb/s, QPSK symbols: 20 Mb/s + 7.6 Mb/s) is achieved over 10-MHz bandwidth.*

Keywords

Derivative-subtractive sampling, discrete multi-tone, optical wireless transmission, sparse compressive sampling, white light emitting diode

1. Introduction

As the 5G mobile environment is implemented, the amount of multi-media data consumed by various smart devices is increasing explosively. In addition, as the number of smart devices accessing 5G networks is rapidly increasing, more 5G access points (APs) and wireless-fidelity (Wi-Fi) APs are being installed [1–3]. Recently, as internet of things (IoT) environments based on artificial intelligence are being created in various building environments such as homes and offices, Wi-Fi is taking its place as the core of wireless communication technology in buildings [4]. However, global academia and industry recognize the steep increase in the share of RF spectrum allocated to Wi-Fi as a potential problem factor in the next-generation mobile network environment to be implemented in the future. Such Wi-Fi congestion occurs in an environment where the demand for wireless resources by various ingenious devices is rapidly increasing. In fact, the shortage of RF frequencies allocated to Wi-Fi has continued to cause the problem of slowing down the Internet in recent years [5]. A new wireless transmission technology that can work synergistically with Wi-Fi is needed to avoid situations such as slowing down the Internet. Among these technologies, visible light communication (VLC) technology has been receiving continuous attention [6–8]. Since this is implemented using light emitting diodes (LEDs) used for lighting, it does not occupy radio resources of Wi-Fi using RF signals. Therefore, it is possible to implement a cooperative relationship with Wi-Fi in order to increase the capacity of the wireless transmission channel. In addition, LEDs are used as lighting in most of the recently constructed buildings, and many innovations have been made in terms of commercialization to the extent that light-fidelity (Li-Fi) products marketed by VLC component development companies have been released [8]. Nevertheless, it should be able to provide an environment (for example, the transmission rate and transmission length) similar to the wireless environment using the existing Wi-Fi in order for the visible light transmission technology to sufficiently fulfill the role of cooperating with Wi-Fi. However, since the yellow phosphorous-based white LED used for lighting has a frequency response of less than 10 MHz, it is quite challenging to implement a transmission rate similar to that of Wi-Fi.

Various techniques have been proposed to increase the transmission rate by overcoming the narrow frequency response of the white LED [9–12]. For example, experimental results of implementing a transmission rate of 10 Gb/s or more using a GaN-based micro-LED were published [9]. P. H. Binh demonstrated the transmission rate of 400 Mb/s in a 30 MHz bandwidth using a ZnSe-based LED [10]. Also, G. Cossu implemented a visible light wireless link with a transmission rate of 3.4 Gb/s at a distance of 10 cm using RGB-LED [11]. On the other hand, Y. Wang presented the transmission rate of 4.5 Gb/s using a modulation technology such as carrierless amplitude phase modulation and RGB-LED [12].

DOI: 10.13164/re.2022.0533

In this paper, we propose a sparse compressive sampling and a derivative-subtractive sampling and use them sequentially in order to transmit the non-return-to-zero-on-off-keying (NRZ-OOK) signal and quadrature phase shift keying (QPSK)-encoded discrete multi-tone (DMT) signal simultaneously using a VLC wireless link based on white LEDs. If the NRZ-OOK signal and the DMT signal are modulated at the same time within the same bandwidth, a mixed signal with the NRZ-OOK signal waveform as an envelope is generated. At first, the length of the mixed signal is reduced (compressed) using sparse compressive sampling. In this way, since more data can be loaded in the empty space created by its reduction (compression), the transmission capacity of the mixed signal can be increased. After the LED light modulated by the compressed mixed signal is transmitted wirelessly, it is recovered to the mixed signal using the L1-minimization technique. In the second step, the NRZ-OOK signal is obtained from the recovered mixed signal using derivative-subtractive sampling. The DMT signal with an analog waveform is recovered by subtracting the obtained NRZ-OOK signal from the recovered mixed signal. We implemented a VLC link and then measured the bit error rate (BER) of NRZ-OOK signal and error vector magnitude (EVM) of QPSK signal decoded from the DMT signal in order to verify the proposed technique.

This paper is organized as follows. Section 2 explains how the proposed technique is implemented using mathematical equations. Section 3 describes how we implement the experimental setup for VLC wireless link to validate the proposed technique. In Sec. 4, both the BER of the NRZ-OOK signal and the EVM of the QPSK signal are presented according to the mutual interference between the two signals, and the received optical power. Section 5 summarizes this paper.

2. Sparse Compressive Sampling and Derivative-Subtractive Sampling for Simultaneous Optical Wireless Transmission of NRZ-OOK and DMT Signal

Figure 1 shows how the compressed DMT signal and the NRZ-OOK signal are simultaneously transmitted and then recovered using the proposed sparse compressive sampling and derivative-subtractive sampling technique. Firstly, as shown in the upper left part of Fig. 1, when the NRZ-OOK signal and the compressed DMT signal are mixed, the NRZ-OOK signal waveform becomes an envelope and the compressed DMT signal is loaded on it. The NRZ-OOK signal can be expressed as (1)

$$S_{1,k}(i)=\sum_{n=0}^{2N-1}\sum_{i=0}^{M-1}A_{(k,n)}\,g\left(\frac{(k-nT)}{T}(i+1)\Delta t_{\mathrm{s}}\right),\qquad g(\alpha)=\begin{cases}1, & \text{for } 0\le\alpha<1\\ 0, & \text{otherwise}\end{cases}\tag{1}$$

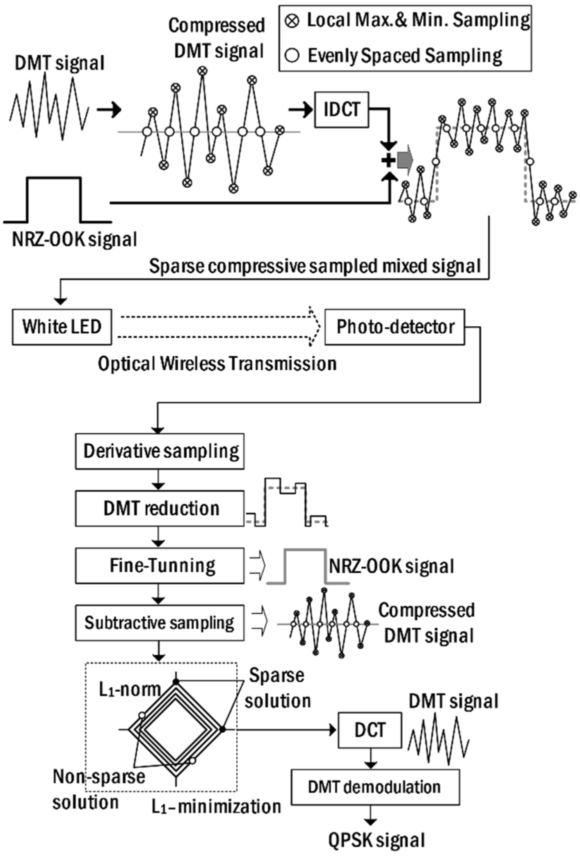

Fig. 1. Simultaneous wireless transmission of NRZ-OOK and DMT signal using sparse compressive sampling and derivative-subtractive sampling.

where $A_{(k,n)}$ is pseudo random bit sequence (PRBS), $g(\alpha)$ is an NRZ-OOK pulse function. α means the input variable of the NRZ-OOK pulse function. k stands for the k^{th} NRZ-OOK symbol consisting of N pulses per symbol. n represents the n^{th} pulse within one NRZ-OOK symbol. T is the period of the NRZ-OOK pulse. i denotes the i^{th} sampling point within one NRZ-OOK pulse.

The DMT signal encoded by QPSK symbols is described as (2)

$$S_{2,k}(i)=\frac{1}{\sqrt{2N}}\sum_{n=0}^{2N-1}C_n\sum_{i=0}^{M-1}\exp\left[\mathrm{j}2\pi n\frac{(k-N_{\mathrm{CP}})}{2N}(i+1)\Delta t_{\mathrm{s}}\right]\tag{2}$$

where C_n is the complex value according to QPSK constellation mapping consisting 4 states. N is the number of DMT subcarriers. N_{CP} is the length of cyclic prefix (CP). Δt_{s} is the sampling period of the digital to analogue (D/A) converter. $S_{1k}(i)$ and $S_{2k}(i)$, with $k = 0,1,\ldots,2N-1+N_{\mathrm{CP}}$, represent the real-valued NRZ-OOK and DMT sequence, respectively.

The procedure of reducing (compressing) the length of the DMT signal using the sparse compressive sampling is as follows. First, sampling points representing local maximum and minimum values are extracted among all sampling points of the DMT signal, and then sampling points are extracted at equal intervals. Here, if the total number of samples of the DMT signal is a_1, the number of sampling the local maximum and minimum points is b_1, and the number of equal sampling is c_1, a_1 is always greater than $b_1 + c_1$. In other words, the number of samples extracted using sparse compressive sampling should be smaller than the total number of samples of the DMT signal. The compressed DMT signal after inverse discrete cosine transform (IDCT) can be expressed as (3)

$$\mathbb{S}_{2,k}(x) = \frac{2}{\sqrt{M}} \sum_{i=0}^{M-1} C(i) \widehat{s_{2,k}(i)} \cos\left(\frac{(2x+1)i\pi}{2M}\right),$$
$$C(i) = \begin{cases} 1/\sqrt{2}, & i = 0 \\ 1, & i > 0 \end{cases} \tag{3}$$

where $\widehat{s_{2,k}(i)}$ is the compressed DMT signal with the length of $b_1 + c_1$ after the sparse compressive sampling. $C(i)$ is the coefficient of IDCT. Therefore, the output signal ($\mathbf{S}_{T,k}$), which is mixed with NRZ-OOK signal and the compressed DMT signal after IDCT, can be written as (4)

$$\mathbf{S}_{T,k} = \mathbf{S}_{1,k} + \mathbb{S}_{2,k}\ . \tag{4}$$

Next, the light from white LED is directly modulated by the mixed signal, $\mathbf{S}_{T,k}$. After optical wireless transmission, the mixed signal, $\mathbf{S}_{T,k}$ is recovered by adding various electrical and optical noises.

After that, the NRZ-OOK signal is extracted from the recovered mixed signal using the derivative-subtractive sampling technique. As shown in (5), the recovered mixed signal vector, $\mathbf{R}_{T,k} = \{r_1, r_2, \ldots, r_m\} \in \mathbb{R}^m$ is composed of an NRZ-OOK signal vector, a compressed DMT signal vector, and various noises vector.

$$\mathbf{R}_{T,k} = \widetilde{\mathbf{S}_{1,k}} + \widetilde{\mathbb{S}_{2,k}} + \mathbf{E} \tag{5}$$

where $\widetilde{\mathbf{S}_{1,k}} = \{\widetilde{s_{1,k(1)}}, \widetilde{s_{1,k(2)}}, \ldots, \widetilde{s_{1,k(m)}}\} \in \mathbb{R}^m$ is the recovered NRZ-OOK signal vector. $\widetilde{\mathbb{S}_{2,k}} = \{\widetilde{s_{2,k(1)}}, \widetilde{s_{2,k(2)}}, \ldots, \widetilde{s_{2,k(m)}}\} \in \mathbb{R}^m$ is the recovered compressed DMT signal vector. $\mathbf{E} = \{e_1, e_2, \ldots, e_m\} \in \mathbb{R}^m$ is the noise vector produced during the optical wireless transmission. The derivative-subtractive sampling technique attenuates portions of the waveform corresponding to sampling points in which the change amount of derivative values between adjacent sampling points in a mixed signal is larger than a set threshold value. This is implemented by taking advantage of the fact that the amount of derivative change between adjacent sampling points of a signal having an analog waveform is much larger than that of a signal with a digital waveform. As mentioned in Sec. 1, the mixed signal shows the waveform in which the compressed DMT signal is loaded on the NRZ-OOK signal waveform that acts as an envelope. Accordingly, as the intensity of the compressed DMT signal having the analog waveform is suppressed, the original waveform of the NRZ-OOK signal is revealed. The compressed DMT signal is obtained by subtracting the recovered NRZ-OOK signal from the mixed signal stored in the buffer.

Equation (6) shows the derivative sampling process in the derivative-subtractive sampling technique

$$y_p(j) = \underset{p \in P_f}{\operatorname{argmin}} \sum_{i \in \mathbb{R}(i)} \left| p(i) - \widetilde{s_{1,k(i)}} \right|^2 \Psi(i,j) + \lambda p_{\mathrm{TV}} \tag{6}$$

where $y_p(j)$ is a polynomial function with degree of f. P_f is the whole space of all polynomial functions below degree of f. $p(i)$ is one of the polynomial functions in the whole space, P_f. λ is the regularization parameter, which governs the shape of NRZ-OOK signal by reducing the intensity of the compressed DMT signal. For your information, as the regularization parameter becomes smaller, the NRZ-OOK signal waveform becomes simplified like a staircase. $\|\ \|_{\mathrm{TV}}$ is total variation (TV) norm, $\|p\|_{\mathrm{TV}} = \int_\Omega |\nabla p| \mathrm{d}x$ with the gradient operator, ∇. $\Psi(i,j)$ is the weight function which is expressed in (7)

$$\Psi(i,j) = \exp\left[-\frac{\sum_{\eta \in \Pi(i)} R_{T,k}(i+\eta) - R_{T,k}(j+\eta)^2 G_\sigma(\eta)}{\rho^2} \right] \tag{7}$$

where Π is the whole set of derivative increments as sampling point of i. ρ is a filtering parameter. G_σ is the Gaussian function with standard deviation of σ. The weight function reflects the similarity between adjacent sampling points in the mixed signal in (7) in order to reduce the error caused by the regularization parameter. For example, in the case of continuously maintaining a large amount of derivative change between adjacent sampling points, the usage of only the regularization parameter reduces the intensity of the corresponding samples below the threshold value. Even the section that changes from 1 (high) to 0 (low) (or 0 to 1) in the NRZ-OOK signal is suppressed, resulting in reducing its signal-to-noise ratio (SNR). The weight function of (7) compensates for these errors. Accordingly, the polynomial function, $y_p(j)$ becomes the recovered NRZ-OOK signal vector ($\mathbf{y}_p \cong \widetilde{\mathbf{S}_{1,k}}$).

Also, the compressed DMT signal, $\widetilde{\mathbb{S}_{2,k}}$ is obtained by subtracting the recovered NRZ-OOK signal vector, y_p from the recovered mixed signal, $\mathbf{R}_{T,k}$ as shown in (8)

$$\widetilde{\mathbb{S}_{2,k}} = \mathbf{R}_{T,k} - \mathbf{y}_p\ . \tag{8}$$

In the process of implementing (6) as an algorithm, the split Bregman method is employed to reduce the computation time because Equation (6) is repeatedly executed on all sampling points of the mixed signal [13].

Next, the compressed DMT signal, $\widetilde{\mathbb{S}_{2,k}}$, can be reconstructed to a DMT signal with the original length using sparse compressive sampling, which is expressed as a product of several matrices using the L1 minimization technique followed by discrete cosine transform (DCT), as shown in (9)

$$\widetilde{\mathbf{S}_{2,k}} = \mathbf{D}\mathbf{b} + \boldsymbol{\epsilon} \tag{9}$$

where, $\widetilde{\mathbf{S}_{2,k}} \in \mathbb{R}^{m \times 1}$ is the noisy DMT signal vector with the original length. $\mathbf{D} \in \mathbb{R}^{m \times m}$ is a basis matrix corresponding to the DCT. $\mathbf{b} \in \mathbb{R}^{m \times 1}$ is the basis vector with a high sparsity. $\boldsymbol{\epsilon} \in \mathbb{R}^{m \times 1}$ is an error vector caused by various electrical and optical noise. The basis matrix, $\mathbf{D}$ is obtained from the compressed DMT signal, $\widetilde{\mathbb{S}_{2,k}}$ transformed by IDCT by continuously updating the sparse matrix, $\Phi \in \mathbb{R}^{n \times m}$, $(n << m)$ until the condition of (10) is satisfied

$$\min_{\mathbf{D},\mathbf{b}} b_1 \text{ subject to } \Phi\widetilde{\mathbb{S}_{2,k}} - \Phi\mathbf{D}b_2 \le \epsilon \ . \tag{10}$$

Therefore, the DMT signal vector, $\widetilde{\mathbf{S}_{2,k}}$ before sparse compressive sampling is obtained using (9) and (10).

3. Experimental Setup

Figure 2 shows the optical wireless link implemented using white LED to experimentally verify that the proposed technique works properly. Waveforms measured at each point from (A) to (G) are presented at the bottom of the optical wireless link. Rectangular boxes with dotted lines are parts that are processed offline using MATLAB®. As shown in the dotted box on the left, a DMT signal encoded by QPSK symbols is implemented by using 1024 subcarriers allocated from DC to 10 MHz. The first 20 of the subcarriers are zero-padded to avoid low spike noise. The CP length was set to 16 considering that the optical wireless link has a property of line of sight and the wireless transmission rate is relatively below 50 Mb/s. The DMT signal waveform created in this way was measured at point (A1) and is shown in the top-left inset at the bottom of Fig. 2. Next, the length of the generated DMT signal is reduced (compressed) by 30% by the sparse compressive sampling. This was measured at point (A2) (the second inset from the top left at the bottom). The transmission capacity of the QPSK signal before sparse compressive sampling was 20 Mb/s, and then it was increased up to 26 Mb/s considering the 30% reduction in length after sampling. The first inset from the top center at the bottom and the first inset from the top right show the spectrograms before and after sparse compressive sampling, respectively. They show the distribution of corresponding frequency components and their intensity distribution with respect to the sampling points. As the color approaches black, it means that the intensity of the frequency components corresponding to the color becomes smaller. As shown in the spectrogram result after sampling, the DMT signal after sampling was sparse because the frequency components corresponding to black are increased after sampling. When an arbitrary signal is sparse, it means that many of its components are zero or close to zero. In general, it is reported that as the sparsity of the signal increases, the error decreases in the process of recovering the signal using the L1 minimization after transmission [14].

Secondly, we generated an NRZ-OOK signal with 4 sampling points per bit using pseudo-random bit sequence (PRBS). Its length was 2^{23}–1. The bandwidth of the NRZ-OOK signal was also 10 MHz, the same as the DMT signal. The waveform of the NRZ-OOK signal was measured at point (B). The compressed DMT signal and the NRZ-OOK signal were combined using an adder and then the mixed signal was loaded on the arbitrary waveform generator (AWG: AWG70002A) sampled at 40 MS/s (measured at point (C), the fourth inset from the top left at the bottom). The output

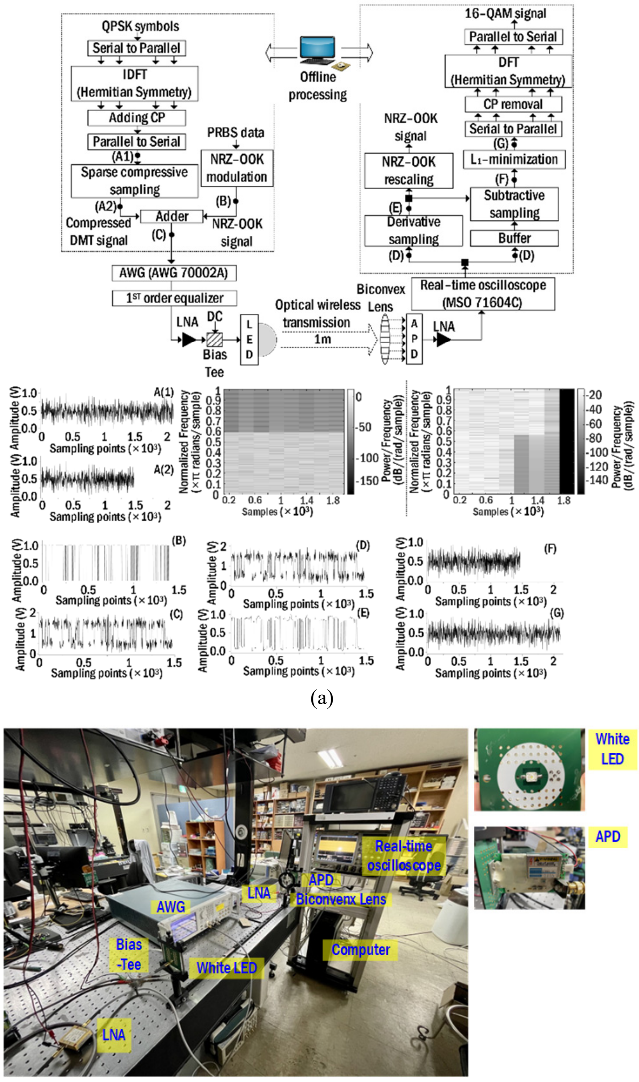

(a)

(b)

Fig. 2. (a) Optical wireless link based on white LED for the simultaneous transmission of sparse sampled DMT signal and NRZ-OOK signal. (b) Photograph of experimental setup.

signal from AWG was equalized using the first order equalizer and then amplified using a low-noise amplifier (LNA: PE15A). After that, the output optical signal from the white LED was directly modulated by the mixed signal, which was biased using the bias-tee. The modulated optical signal was transmitted wirelessly over a distance of 1 meter to the avalanche photo diode (APD, Hamamatsu C5331-11) after passing through the biconvex lens. The link distance was determined by measuring the length from the white LED to the APD. Since the light from the white LED is diffused, as the link distance increases, the intensity of the light received at the APD decreases in inverse proportion to the square of the link distance. Therefore, when the transmission distance increases, both the BER of the NRZ-OOK signal and the EVM of the QPSK signal increase due to the deterioration of the receiver sensitivity of the optical wireless link.

The white LED was a product of OSRAM® (LUW W5AM) manufactured in surface mount technology (SMT) package type. It was implemented based on ThinGaN. It was reported that its light output was 116 lm and a viewing angle of 50% light output was 170°. Also, the used lens was a Thorlabs product (LB1723-A). Its shape was biconvex type, and the focal length was 60 mm. Its diameter was 50.8 mm. The wavelength passband of light was 350 to 700 nm. The used bias-tee is a product of Mini-Circuits® (ZFBT-6GW-FT+) and has a frequency band of 100 kHz to 6 GHz. The insertion loss is 0.15 dB and the voltage standing wave ratio (VSWR) is 1.06:1. The maximum power of the input RF signal is 30 dBm, and the maximum voltage at DC port was 30 V.

The intensity of light measured at the APD was 300 lx. The mixed signal from APD was captured by a real-time oscilloscope (MSO 71604C) sampled at 120 MS/s (measured at point (D), the second inset from the bottom center). The captured mixed signal was equally divided into two parts. One was temporarily stored in the buffer, and the intensity of the components corresponding to the compressed DMT signal in the other was reduced by using the derivative sampling mentioned in (6) and (7). The regularization parameter of (6) was set to 2. The recovered NRZ-OOK signal waveform was measured at point (E). The compressed DMT signal was obtained by subtracting the recovered NRZ-OOK signal from the mixed signal stored in the buffer using subtractive sampling. The compressed DMT signal was obtained by subtracting the recovered NRZ-OOK signal from the mixed signal stored in the buffer using subtractive sampling (see the waveform measured at point (F)). Furthermore, the intensity of the recovered NRZ-OOK signal before sampling was finely adjusted according to the input signal level in order to minimize errors occurring in the subtractive sampling. The compressed DMT signal was recovered to the DMT signal with the original length using the L1 minimization (see the waveform measured at point (G)). The QPSK symbols were obtained from the recovered DMT signal using the DMT demodulation. In this paper, we focused on conceptually verifying whether the proposed technique works appropriately rather than trying to obtain the maximum transmission capacity using the proposed technique. Thus, we verified the proposed technique by implementing a relatively low optical wireless link.

4. Results and Discussions

Figure 3 shows the BER of the NRZ-OOK signal and the EVM of QPSK symbols, which were repeatedly measured while reducing the length of the DMT signal from 0% to 45% compared to the original signal length using the sparse compressive sampling technique. The open squares represent the BERs of the NRZ-OOK signal when the proposed technique is not applied, and the filled squares represent BERs measured using the proposed technique. The open triangles show the EVM of the QPSK signal. The insets of Fig. 3 show the eye patterns of the NRZ-OOK signal and the constellation of the QPSK signal when the compression ratio was 30%.

As shown in Fig. 3, the increase in EVM of QPSK symbols was observed as the compression ratio was increased.

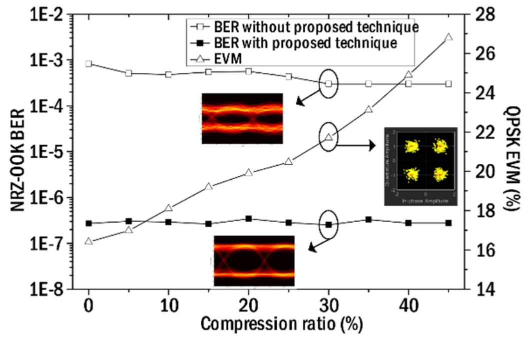

Fig. 3. Measured NRZ-OOK BERs and QPSK EVMs against the compression ratio of DMT signal.

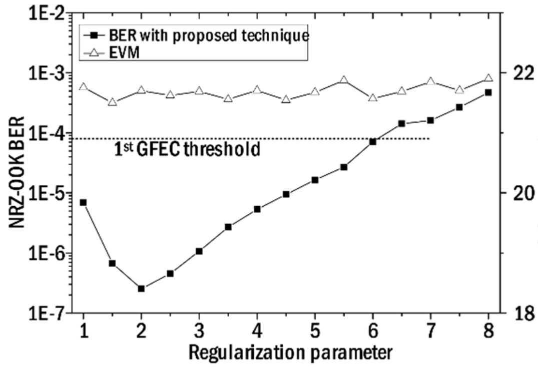

(a)

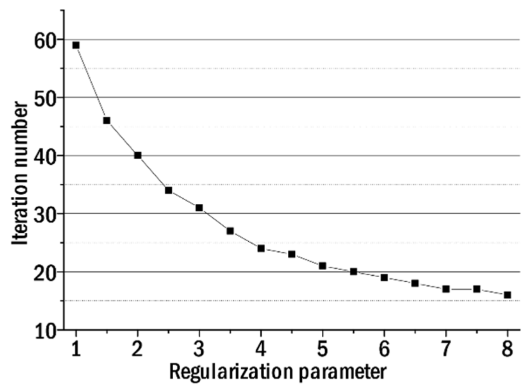

(b)

Fig. 4. (a) BER change of NRZ-OOK signal and EVM change of QPSK symbols against the regularization parameters. (b) Iteration number of derivative-subtractive algorithms against the regularization parameter.

Nevertheless, the BER of the NRZ-OOK signal maintained a constant value regardless of the compression ratio. These results can be explained as follows. Since only the length of the DMT signal is compressed and then transmitted by using the sparse compressive sampling, errors due to compression increase in the reconstruction process. The BER of the NRZ-OOK signal was observed to be reduced from 3×10^{-4} to 2.5×10^{-7} (based on a 30% compression ratio) using the derivative-subtractive sampling. Furthermore, the BERs after the derivative-subtractive sampling were measured repeatedly between 2×10^{-7} and 3×10^{-7} in other compression ratios. Therefore, it can be said that the sparse compressive sampling technique only affects the transmission performance of the DMT signal encoded by the QPSK symbols. For reference, taking into account the first-generation generic forward error correction (GFEC) threshold (BER: 8×10^{-5}, EVM: 24.6%), it is possible to transmit by reducing the length of the DMT signal up to 38%. In this case, it means that it is possible to secure 37.6-Mb/s transmission capacity (NRZ-OOK signal: 10 Mb/s, QPSK signal: 20 Mb/s + 7.6 Mb/s) based on 10 MHz bandwidth. In other words, this means that the transmission capacity can be increased by about 3.76 times compared to the occupied bandwidth.

Figure 4(a) shows the BER of the NRZ-OOK signal and the EVM of the QPSK symbol, which were repeatedly measured while increasing the regularization parameter mentioned in (6) from 1 to 8. Figure 4(b) shows the number of iterations of the differentiation-subtraction algorithm corresponding to each regularization parameter. As shown in Fig. 4(a), the BER of the NRZ-OOK signal was minimized when the regularization parameter was 2. On the other hand, the EVM of the QPSK signal was measured between 21.5% and 22% regardless of the regularization parameter. This means that the derivative-subtractive sampling technique only affected the transmission performance of the NRZ-OOK signal. It was also observed that it was possible to transmit the NRZ-OOK signal even if the regularization parameter increased up to 6 based on the 1st GFEC BER threshold. As shown in Fig. 4(b), the number of iterations was reduced as the regularization parameter increased. This is because, as the regularization parameter increases, the second term in (6) quickly converges below a predetermined threshold value. As shown in Fig. 4(a), the number of iterations can be reduced to 19 because it is possible to transmit when the regularization parameter was 6.

Figure 5 shows the BER of the NRZ-OOK signal and the EVM of the QPSK symbol according to the change in the received light intensity (unit: lx) after 1-m optical wireless transmission. Figure 5(a) shows the BERs of NRZ-OOK signal, which were repeatedly measured before and after using the proposed technique while increasing the received light intensity from 210 lx to 440 lx. Filled squares represent the BER measured without the proposed technique, and open squares represent the measured BER when the proposed method is not used. In the case of applying the proposed technique, the BER floor was observed between 1×10^{-7} and 2×10^{-7} when the received light intensity was 300 lx or more. This is because the minimum BER we can obtain is 1.19×10^{-7} due to the PRBS length of 2^{23}–1. In the end, even if the received light intensity increases more than 450 lx, the BER does not decrease below 1.19×10^{-7}. In the case of the NRZ-OOK signal, it was observed that the successful transmission of the NRZ-OOK signal was possible only when the received light intensity was 220 lx or more (based on the 1st GFEC threshold). Also, as shown in Fig. 5(b), it can be seen that QPSK symbol transmission is possible only when the received optical power is 280 lx or more based on the 1st generation GFEC threshold. Therefore, the received light intensity should be greater than 280 lx in order to transmit both the NRZ-OOK signal and the DMT signal at the same time.

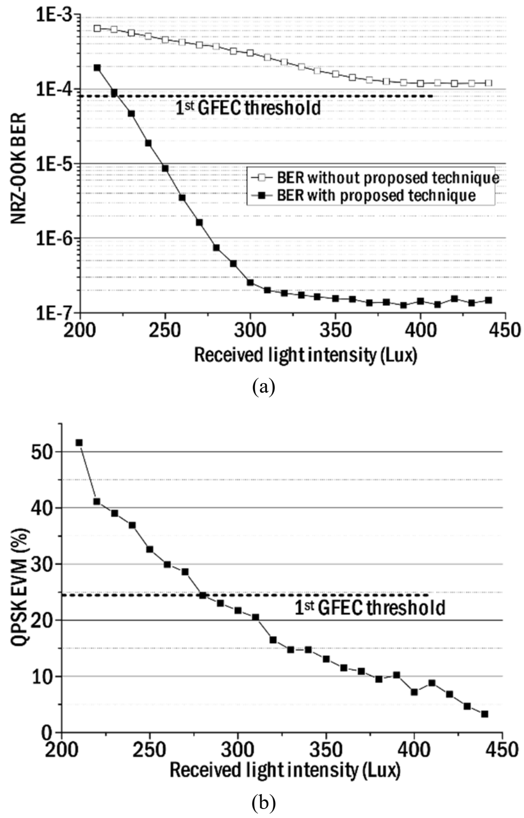

Fig. 5. (a) BER change of NRZ-OOK signal and (b) EVM change of QPSK symbols against the received light intensity.

Since the NRZ-OOK signal and the DMT signal are simultaneously transmitted using a bandwidth of 10 MHz, mutual interference may inevitably occur. Accordingly, it is necessary to find out how the mutual interference between them affects the transmission performance before and after using the proposed technique. Figure 6 shows how the BER of the NRZ-OOK signal and the EVM of the QPSK symbol change according to the change in the ratio of the DMT signal to the NRZ-OOK signal. The ratio of the DMT signal to the NRZ-OOK signal is defined as the value obtained by dividing the power of the DMT signal by the power of the NRZ-OOK signal. It is expressed as B/A in the figure at the bottom of Fig. 6. Open squares represent the case where the proposed technique is not applied, and filled squares represent the BER when the proposed technique is applied. Open triangles correspond to the EVM of the QPSK symbol. It was found that the BER of the NRZ-OOK signal increased as the ratio of the DMT signal increased when the proposed technique was not employed. This is because the SNR of the NRZ-OOK signal was reduced as the intensity of the DMT signal occupying the same bandwidth of went up. If the proposed technique is not used, it becomes difficult to transmit the NRZ-OOK signal at the ratio of the DMT signal greater than 0.8. In the case of using the proposed technique, the BERs of the NRZ-OOK signal were measured close to the minimum BER (1.19×10^{-7}) corresponding to the PRBS length of 2^{23}–1 since the intensity of the DMT signal was reduced by the derivative-subtractive sampling. In addition,

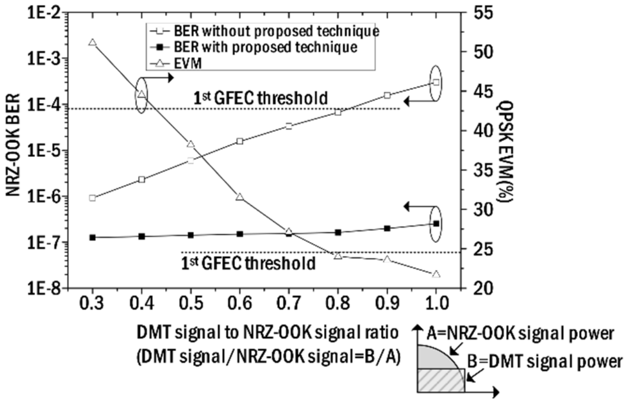

Fig. 6. BER change of NRZ-OOK signal and EVM change of QPSK symbols against NRZ-OOK signal to DMT signal ratio.

the EVM of QPSK symbols became small because the SNR of the DMT signal was improved as the ratio of the DMT signal increased. It was found that it was possible to transmit QPSK symbols at the ratio of DMT signal was greater than 0.8. Therefore, it could be seen that it was possible to transmit NRZ-OOK and QPSK symbols at the same time when the ratio of the DMT signal was 0.8 or more.

Figure 7 shows the measured BER of NRZ-OOK and EVM of the QPSK signal while changing the signal-to-noise ratio of the input mixed signal from 15 dB to 40 dB. At this time, the compression ratio was set to 30% and the light intensity received from the APD was 300 lx. Open squares show the BER of the NRZ-OOK signal before the proposed technique and filled squares show the BER after the proposed technique. Open triangles show the EVM of the QPSK signal when the proposed technique is used. We found that it was possible to transmit the NRZ-OOK signal in the overall SNR range from 15 dB to 40 dB based on the threshold of the 1st generation GFEC in the case of using the proposed technique. On the other hand, in the case of the QPSK signal, a successful transmission was observed only when the SNR of the input mixed signal is about 33 dB or more considering the 1st generation GFEC threshold.

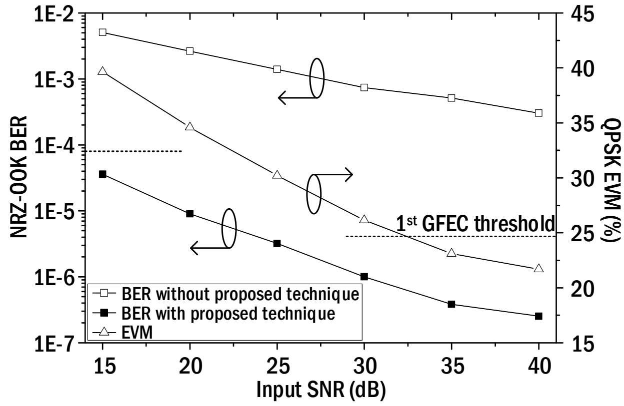

Fig. 7. BER change of NRZ-OOK signal and EVM change of QPSK symbols against the SNR of input mixed signal.

5. Conclusion

A new technique for simultaneously transmitting two signals having different waveforms within the same bandwidth has been proposed in order to increase the transmission capacity of an optical wireless transmission link based on visible LED. As two signals with different waveforms, an NRZ-OOK signal with a digital waveform and a DMT signal encoded by a QPSK symbol with an analog waveform were used in the optical wireless link. In this paper, a sparse compressive sampling technique based on compressive sensing was proposed in order to reduce the length of the DMT signal, and a derivative-subtractive sampling technique was also proposed to separate two different signals after optical and wireless transmission. We reduced the length of the DMT signal up to 38% using the sparse compressive sampling technique. In addition, in the case of the NRZ-OOK signal, a BER close to the minimum BER (1.19×10^{-7}) corresponding to the PRBS length (2^{23}–1) was measured using the derivative-subtractive sampling technique, and in the case of the QPSK symbol, the EVM was measured below the first-generation GFEC threshold (24.6%). As a main experimental result, a transmission capacity of 37.6 Mb/s was secured in an optical wireless transmission with a physical bandwidth of 10 MHz.

Acknowledgments

This work was supported by 2022 Research Fund of Myongji University.

References

[1] WU, X., SOLTANI, M. D., ZHOU, L., et al. Hybrid LiFi and WiFi networks: A survey. *IEEE Communications Surveys & Tutorials*, 2021, vol. 23, no. 2, p. 1398–1420. DOI: 10.1109/COMST.2021.3058296

[2] CHOWDHURY, M. Z., HASAN, M. K., SHAHJALAL, M., et al. Optical wireless hybrid networks: Trends, opportunities, challenges, and research directions. *IEEE Communications Surveys & Tutorials*, 2020, vol. 22, no. 2, p. 930–966. DOI: 10.1109/COMST.2020.2966855

[3] CISCO. *Cisco Visual Networking Index: Forecast and Trends, 2017–2022*. Cisco, San Jose, CA, USA, Rep., Nov. 2018.

[4] ZHANG, D., ZHOU, Z., MUMTAZ, S., et al. One integrated energy efficiency proposal for 5G IoT communications. *IEEE Internet of Things Journal*, 2016, vol. 3, no. 6, p. 1346–1354. DOI: 10.1109/JIOT.2016.2599852

[5] DE VRIES, J. P., SIMIĆ, L., ACHTZEHN, A., et al. The Wi-Fi "congestion crisis": Regulatory criteria for assessing spectrum congestion claims. *Telecommunications Policy,* 2014, vol. 38, no. 8–9, p. 838–850. DOI: 10.1016/j.telpol.2014.06.005

[6] POHLMANN, C. Visible light communication. In *Proceedings of Seminar Kommunikationsstandards der Medizintechnik*, 2010, p. 1–14.

[7] MATHEUS, L. E. M., VIEIRA, A. B., VIEIRA, L. F. M., et al. Visible light communication: Concepts, applications and challenges. *IEEE Communications Surveys & Tutorials*, 2019, vol. 21, no. 4, p. 3204–3237. DOI: 10.1109/COMST.2019.2913348

[8] HAAS, H., YIN, L., WANG, Y., et al. What is LiFi? *Journal of Lightwave Technology*, 2016, vol. 34, no. 6, p. 1533–1544. DOI: 10.1109/JLT.2015.2510021

[9] ISLIM, M. S., FERREIRA, R. X., HE, X., et al. Towards 10 Gb/s orthogonal frequency division multiplexing-based visible light communication using a GaN violet micro-LED. *Photonics Research*, 2017, vol. 5, no. 2, p. A35–A43. DOI: 10.1364/PRJ.5.000A35

[10] BINH, P. H., HUNG, N. T. High-speed visible light communications using ZnSe-based white light emitting diode. *IEEE Photonics Technology Letters*, 2017, vol. 28, no. 18, p. 1948–1951. DOI: 10.1109/LPT.2016.2578964

[11] COSSU, G., KHALID, A. M., CHOUDHURY, P., et al. 3.4 Gbit/s visible optical wireless transmission based on RGB LED. *Optics Express*, 2012, vol. 20, no. 26, p. B501–B506. DOI: 10.1364/OE.20.00B501

[12] WANG, Y., HUANG, X., TAO, L., et al. 4.5-Gb/s RGB-LED based WDM visible light communication system employing CAP modulation and RLS based adaptive equalization. *Optics Express*, 2015, vol. 23, no. 10, p. 13626–13633. DOI: 10.1364/OE.23.013626

[13] GOLDSTEIN, T., OSHER, S. The split Bregman method for L1-regularized problems. *SIAM Journal on Imaging Sciences*, 2009, vol. 2, no. 2, p. 323–343. DOI: 10.1137/080725891

[14] DONOHO, D. L. Compressed sensing. *IEEE Transactions on Information Theory*, 2006, vol. 52, no. 4, p. 1289–1306. DOI: 10.1109/TIT.2006.871582

About the Authors ...

Yong-Yuk WON (corresponding author) was born in South Korea. He received the B.S. and M.S. degrees in Electrical and Electronic Engineering from Yonsei University, Seoul, South Korea, in 1997 and 1999, respectively, and the Ph.D. degree in Electrical and Electronic Engineering from Yonsei University, South Korea, in 2008. From 1999 to 2002, he was with the Optoelectronics Laboratory, Samsung Electronics, where he was involved in research and development on optical devices. He is currently an Assistant Professor with Myongji University, South Korea. His current research interests include passive optical networks, visible light communication, optical devices, and optical systems for communications.

Sang Min YOON was born in South Korea. He received the B.E. and M.E. degrees in Electronics Engineering from Korea University, Seoul, South Korea, in 2000 and 2002, respectively, and the Dr.Ing. degree with Informatik, TU Darmstadt, Darmstadt, Germany, in 2010. He then joined the Digital Human Research Center, Advanced Industrial Science and Technology (AIST), Tokyo, Japan, as a Postdoctoral Researcher. He was a Researcher in the areas of face recognition and video surveillance with the Samsung Advanced Institute of Technology (SAIT), from 2002 to 2005. He has been with the College of Computer Science, Kookmin University, South Korea, as an Associate Professor, since 2012. His main interests include human motion analysis and understanding, 3D model retrieval, and human-computer interface (HCI).